Proceedings of the 6th International Conference on the Application of Physical Modelling in Coastal and Port Engineering and Science (Coastlab16)
Ottawa, Canada, May 10-13, 2016

NUMERICAL SIMULATIONS OF COMPRESSIBILITY EFFECTS IN FREE-SURFACE FLOW RESULTING FROM WAVE IMPACTS ON AN IDEALIZED SEAWALL

OLIVIER G. TREMBLAY, JANNETTE B. FRANDSEN

Institut national de la recherche scientifique, Canada, olivier.gauvin-tremblay@ete.inrs.ca

ABSTRACT

This study aims to investigate the free-surface flow involved in different wave impact types to achieve an improved insight in the design of seawalls and coastal infrastructures subjected to moderate and storm wave conditions. Local pressure as well as forces and overtopping quantities are of interest in designing such walls. Since forces and pressures highly vary depending on wave form at impact and amount of air trapped under breaking waves, it is necessary to achieve an accurate modeling of the breaking processes. Herein, a comparison between numerical results from a CFD model and experimental recordings conducted in the Quebec Coastal Physics Laboratory large scale flume is presented. The CFD model performance is tested to investigate the more fundamental mechanisms of the underlying processes and to assess real conditions around seawalls to facilitate design process. The preliminary results are based on 2D compressible flow simulations, as air-pocket physics and air-water interactions are important in predicting the pressure evolution on a seawall. Results show that compressible flow simulations present the same trend than experiments in terms of impact type, predict the same order of magnitude in pressure and that they can capture interesting characteristics such as air-pocket oscillations.

KEWORDS: Wave impact, compressibility effects, free-surface flow, numerical simulations, large-scale experiment

1 INTRODUCTION

In the development of designing coastal infrastructures facing harmful marine events, failure events are known to have happened from which it can be observed our existing understanding about wave impact on walls is not sufficient. Actually, water and air motion as well as pressure distributions on seawalls due to violent impacts are highly complex. Air-water interaction and other nonlinearities thereby bring us to investigate more deeply the physics of the impact process, including the compressibility effects.

Those efforts are made in order to develop prediction tools for wave loadings on structures such as walls and deflectors in continuity with Tremblay *et al.* (2015) and to insure proper design (even though there are several studies about the fundamental aspect). A robust knowledge has been developed for wave forces on offshore infrastructures (Lighthill, 1986 and Sarpkaya, 2010), but these ones are subjected to waves in deep water condition. In fact, shoaling processes transport waves to break at or near the wall, which involves highly non-linear behaviors with entrained air causing compressibility effects.

In the literature, several contributions can be found. It has been established that the way a wave strikes a vertical wall, i.e. its shape and the type of breaking, influences the resulting impact (Peregrine, 2003) and contains considerable variability. Bagnold (1939) tested different shapes at the wall resulting in different amount of trapped and entrained air. The different impacts lead to various peak pressure amplitudes. In fact, Bagnold showed with his small scale experiments in a flume 3.66 m long, 1.22 m deep and 0.53 m wide that the case involving almost no trapped air present the highest pressure peaks. This case is often referred to as the flip-through impact type.

Guilcher *et al.* (2014) have conducted near full scale numerical simulations to study the different phases of the impact and the effects of different wave shapes and amount of entrapped air at the impact. They demonstrated that their SPH solver was able to reproduce such physics and that this type of tool is able to bring more information to experiments. It also comes out that compressibility effects should be taken into account in the assessment of breaking wave loadings.

Also with a gridless method, Khayyer et al. (2009) show that numerical simulation is a possible way to study wave impacts and to do some predictions in pressure evolution. Despite the fact that lagrangian methods are suitable in dealing

with free-surface flows, the VOF technique also presents reasonable agreement with experiment (Mayer *et al.*, 2005), provided that proper inlet (initial) conditions are used (Mokrani *et al.*, 2013).

Hofland *et al.* (2010) used large scale experiments to investigate wave impacts on vertical walls. They also obtained the greatest pressure peaks with the flip-through impact. In their two-hundred-meter-long and seven-meter-deep flume, a peak as high as 2.7 MPa was observed within a duration of less than a millisecond. Indeed, time duration is likely to be an important parameter as the impulse on walls is a more relevant metric (Peregrine, 2003) since there is great variability in wave impacts.

In 2007, Bullock *et al.* (2007) also used large scale facilities to study the role played by the entrapped air. Cuomo *et al.* (2010) also conducted large scale experiments and compared the results with prediction (empirical and analytical) formulae on impact forces and overturning moments. The authors distinguished two types of wave load on structures: short-duration impact or "quasi-static" load, depending on the natural frequency of the structure. In fact, loads can be considered as quasi-static if the wave-impact time duration is much longer than the natural period of vibration.

It is for the same reasons that Hattori *et al.* (1996) had studied dynamic responses of an elastic seawall. They noted that the vibrational response of the non-rigid structure depended on the impact type, that is a single peaked load or a more damped pressure oscillation load. These kinds of observation also allow differentiating wall vibration from pressure oscillations due to air trapping within the pressure sensors.

In short, local pressures as well as forces and overtopping quantities are of interest in designing such walls. Since forces and pressures highly vary depending on wave form at impact and amount of air trapped under breaking waves, it is necessary to achieve an accurate modeling of the breaking processes. Compressibility effects must also be taken into account in the numerical model as it has been emphasized that the physics related to air pockets and air-water interactions are important in understanding and predicting the pressure evolution on a seawall (Bredmose *et al*., 2009).

2 VALIDATION MATERIAL OF LARGE SCALE TESTS

One of the motivations for the present numerical work is to support experimental study and help in designing a deflector for the physical model scale tests. It is why experiments serve as a point of comparison for the numerical simulations. The experimental part of the study was conducted in the large scale flume of the new Quebec Coastal Physics Laboratory in Canada (Figure 1). The flume is 122 m long, 5 m depth and 5 m wide, with an idealized seawall installed at the top end (Figure 2), after a 1:10 beach slope made of mixed cobble-gravel-sand. The seawall is 2.47 m high and sets in three different parts. The central part is the instrumented one and can hold 55 different sensors within threaded holes equally spaced on a 25.4 mm tick aluminum plate. This plate is reinforced by steel beams that also act as part of ten contact point supports on the back flume wall.

Twenty-five sensors take place on the plate in this experiment. Among these, there are 20 PCB and 5 Kistler pressure sensors. All sensors are recording at a sampling rate of 125 kHz. In order to have a complete vertical profile and some 3D information, pressure sensors are distributed over the wall height in three columns. Finally, there are a set of cameras installed in the flume to capture the wave shape as it impacts the wall and outside the flume to get a general picture and to measure jet height and velocity.

Figure 1. Impact on a seawall in the Quebec Coastal Physics Laboratory facilities.

To obtain wave impact near the middle of the plate, water depth h_0 is set to 3.8 m in the flume (intermediate water depth) and wavetrains made up of ten crests are launched from still water condition. Wave period T is about six seconds and wave height H ranges from 0.85 to 1.3 m to get different types of impact. The piston type wavemaker is configured to generate waves with a variety of different initial waveforms. More information is available in Frandsen *et al*. (2015; 2016).

Figure 2. The central instrumented wall is mainly composed of an aluminium plate with 25 pressure sensors (in red) installed. A flat steel plate (right picture) is welded at the bottom to prevent scouring.

3 NUMERICAL MODEL

As to deepen our understanding of the wave impact process, it is found that numerical modeling may be a guiding complementary approach. For this reason and for validation purpose, the experimental setup is therefore reproduced exactly in the numerical model.

In this study, the assumption of treating the wall as a rigid plate is made and fluid-structure interaction physics is treated as a decoupled process. To check this assumption, some modal analyses of the seawall structure have been conducted. This type of information is interesting in order to study the interaction of the wave and the entrapped air with the wall. Table 1 presents the first five modes natural frequencies of the wall. In comparison with the time-duration of an impact (around 1 ms as shown in the next section), one can see that the structure responds more slowly than the excitation. Then, it should be expected that fluid-structure coupling is weak.

Table 1. Natural frequencies of the first five modes of vibration associated to the wall, as it is installed in the flume.

Mode	Frequency [Hz]
1	74.7
2	81.3
3	108.8
4	150.5
5	168.9

Using commercial code ANSYS Fluent, 2D incompressible and compressible URANS multiphase flow calculations have been conducted. Two-dimensional simulations are a good starting point since the flow appears to be 2D. Compressible 2D Navier-Stokes equation (with turbulence modeling), along with continuity equation, can be found in the form:

$$\frac{D(\rho \boldsymbol{u})}{Dt} = -\nabla p + \rho g + \mu \nabla^2 \boldsymbol{u} - \nabla \cdot (\rho \overline{u'v'}) \tag{1}$$

$$\frac{D\rho}{Dt} + \rho \nabla \cdot \boldsymbol{u} = 0 \tag{2}$$

In the compressible flow simulations, fresh water (as in the experimental part) is treated as an incompressible liquid (ρ is constant) and air is treated as an ideal gas. The energy equation must be solved to track density fluctuations in air:

$$\frac{\partial}{\partial t}(\rho E) + \nabla \cdot \big(\boldsymbol{u}(\rho E + p)\big) = \nabla \cdot (k \nabla T) \tag{3}$$

$$E = c_p T - \frac{p}{\rho} + \frac{|\boldsymbol{u}|^2}{2} \tag{4}$$

In order to capture the free-surface, a VOF technique is used, since it allows getting the smooth interface between water and air (Hirt *et al*., 1981). However, this type of multiphase model has some limitations in capturing small structures (air bubbles, water drops).

The free-surface capturing is based on the Geo-Reconstruct explicit algorithm (ANSYS, 2014) and the SIMPLE algorithm is used for the pressure-velocity coupling. Spatial discretization schemes are of second order and that for temporal discretization is only of first order, since the VOF method used limits us at this order. The time step is chosen sufficiently

small so that temporal errors could be neglected. A time step of 1.667×10^{-3} T (T is the wave period) is applied initially to simulate the propagation of the waves through the flume while a time step of 1.667×10^{-5} T is used during the breaking process and the impact. A smaller time step has been tried (6.67×10^{-6} T) but no difference was seen in term of peak pressure calculated. The *k-ε* model is chosen for turbulence modeling (to solve last term of Equation 1), so a wall function is used to account for the no-slip condition on the simple flat boundaries.

The flow domain and the boundary conditions applied are indicated in Figure 3. Rigid boundaries with no-slip conditions are used for the flume bottom, the beach slope and the idealized seawall. A wave profile within a "velocity-inlet" condition type is imposed at the inlet. From the available wave theories in Fluent, a 5th order Stokes formulation is used. Other parameters, such as depth (h_0=3.8 m) and wave period (T=6 seconds) are constant and identical to the experimental part. Indeed, one of the objectives of these simulations is to reproduce the large scale experiments for later comparison. Measured Froude number associated to the incoming wave at the beach toe ($Fr = V_{ref}/\sqrt{gh_0}$) is 0.18 for the H=1.3 m numerical case whereas it is equal to 0.14 in the experiment. A "pressure-outlet" (hydrostatic profile) is assumed behind the wall to stabilize the calculations and allow normal air movement within the domain. Other boundaries are set as slip walls. It should be noted at Figure 3 the "chimney" above the seawall to account for water jet associated with the splash.

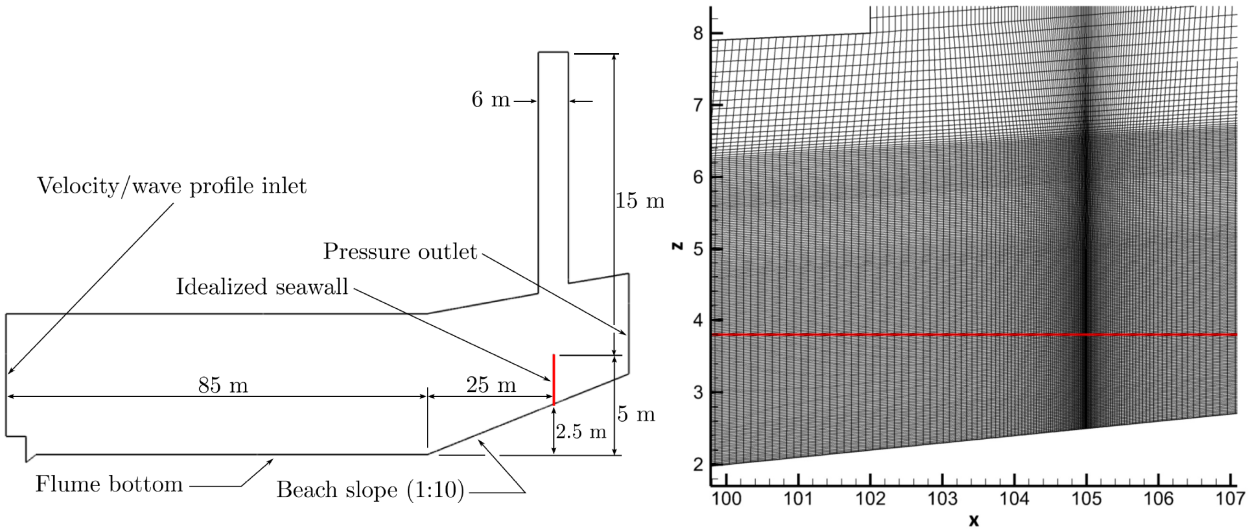

Figure 3. On the left, numerical domain for the wave impact calculations illustrating the boundary conditions applied. Horizontal scale is shrunk by a factor of four compared to the vertical scale. On the right, spatial discretization around the seawall associated to the selected mesh. Still water level is illustrated by a red line at z=3.8 m and the wall is localized at x=105 m.

To capture properly the physics of the problem, a mesh independence study have been done with a slip condition on the wall and incompressible water as an initial guess. From coarse to fine, four grids have been tested with the same case, i.e. h_0=3.8 m, T=6 s and H=1.3 m, and pressure peaks have been measured during impact. Along the process, cells are mostly refined in the impact region (near the wall) both in height and in length, although cells over the beach slope are also refined to improve accuracy of the inlet conditions. A comparison of the meshes is shown in Table 2. The mesh of 105 430 cells is inaccurate. The two finer grids give a pressure peak inside a range less than one percent and they show the same duration time (about 0.5 ms). Therefore, it is decided to choose the mesh no 3 (Figure 3) as an initial guess for the present study.

For this grid, longitudinal length of cells in the breaking region is about λ/200 to insure a good capture of the incoming waves (the wave length λ is about 35 m) and cell height is set around H/50 in the free-surface region to get a sharp interface. Since a no-slip condition will be used in this calculation, cell length (perpendicular to the wall) in the seawall region have to be shortened. It is essential to capture adequately the jet propagating upward and to calculate proper shear stress within the boundary layer. With a *k-ε* turbulence model, it is recommended to keep the first cell y^+ over 30-50 (ANSYS, 2014 and Launder *et al*., 1974)[1] . For the present simulations, with $0.0005 < \Delta x < 0.003$ m at the wall, maximum y^+ values range from 400 to 4500, keeping in mind that the Reynolds number $Re = V_{max} h_{wall}/\nu$ (based on the maximum jet velocity and the wall height) is greater than 1×10^8. In the same region, $\Delta z \approx 0.015$ m, yielding a CFL number below 1. More investigation on grid sensitivity and boundary layer treatment for jet velocities have to be done.

[1] y^+ is the dimensionless wall distance used to study boundary layers. At every (large) Reynolds number, viscous sublayer is contained within $y^+ < 10$. Since *k-ε* turbulence model uses a wall function, the first cell has to stand outside the viscous sublayer, in the "log law" region which is above y^+ = 30-50.

Table 2. Pressure peaks associated to the mesh independence study. Constant wave parameters are h_0=3.8 m, T=6 s and H=1.3 m.

Mesh	Number of cells	P_{peak} [kPa]
1	105 430	787
2	181 570	3930
3	219 930	2936
4	275 630	2953

Hereafter, results are presented for different inlet wave heights, ranging from 1.2 to 1.5 m, throughout incompressible and compressible flow simulations. In the present work, we are studying the second impact at the wall as it yields peak wall pressure (successive impacts may also produce important pressures, but it is not part of the scope of the present numerical study). Simulations have been run in parallel processing (single node) and each one takes about 72 core hours to complete.

4 NUMERICAL PREDICTIONS

As a first step in analyzing the different results from experimental and numerical tests, the maximum local peak pressures recorded from the test series are presented in Table 3 as a function of the amount of entrained air. It can be seen that the three methods exhibit very high pressures for the flip-through case, in the order of 3 MPa. However, discrepancies of about 50% exist between the different methods. The flip-through impact is a particular (limit) case between sloshing impact (the wave did not brake) and air-pocket impact (the wave became a plunging breaker) and is thus sensitive to any variation (difference) in the inlet conditions.

Table 3. Maximum local peak pressures on the wall for different types of impact.

Type of impact	Experimental	Numerical	
		Incompressible	Compressible
	[kPa]	[kPa]	[kPa]
Sloshing	248	237	-
Flip-through	3340	2572	4646
Small air-pocket	916	-	-
Large air-pocket	624	3440	415

Slight differences can affect the wave transformation and then produce a wide range of peak pressure on the wall. For example, compressible and incompressible simulations have “transition moments” from the start time step to the finer time step slightly different, enough to influence the wave transformation downstream. Moreover, there exist differences in the inlet between the experiments and the simulations. The experimental tests use a deforming and absorbing bed made of a cobble-gravel-sand mix whereas the numerical model uses a smooth and rigid bed. Besides the inlet aspect, it should also be noted that resolution on the wall is very different between the numerical and the experimental part. Along the wall, the first one gives (calculates) pressure every 0.015 m while the second one gives pressure information from sensors every 0.2 m. So, all the pressure peaks may have not been captured in the experiments. Therefore, the maximum local peak pressure reported in the experiments may not be the highest pressure generated.

To validate if the discrepancies observed in the maximum peak pressure for the flip-through impacts come entirely from differences in the inlet conditions or in the resolution, a comparison of the pressure evolution and distribution can be made. Figure 4 shows a comparison of wall pressure at five locations (experimental setup summarily illustrated in Figure 4) between an experimental flip-through impact and a compressible numerical flip-through impact exhibiting similar free-surface shapes before reaching the wall (the experimental wave is actually a little bit bigger). It can be noted that impact durations are very similar, as well as pressure curve evolution (aspect). Maximum pressure can be found near the still water level (in C6) in both cases. The experimental data are more noisy and sometimes more peaky (red and green lines). Outside the fact that the compressible simulation shows a higher peak pressure, it tends to reproduce properly the general behavior of the impact.

From Table 3, it can also be seen that incompressible numerical and experimental results do not match for large air-pocket impact. Incompressible simulations show too high peak pressures. Those pressures are in fact reached in the air-pocket region, almost everywhere within it. Figure 5 shows the difference between the pressure reached in the air-pocket region and that reached at the crest impact position. The first one has a very short rising time and goes very high whereas the second has a pressure peak almost seven times less important.

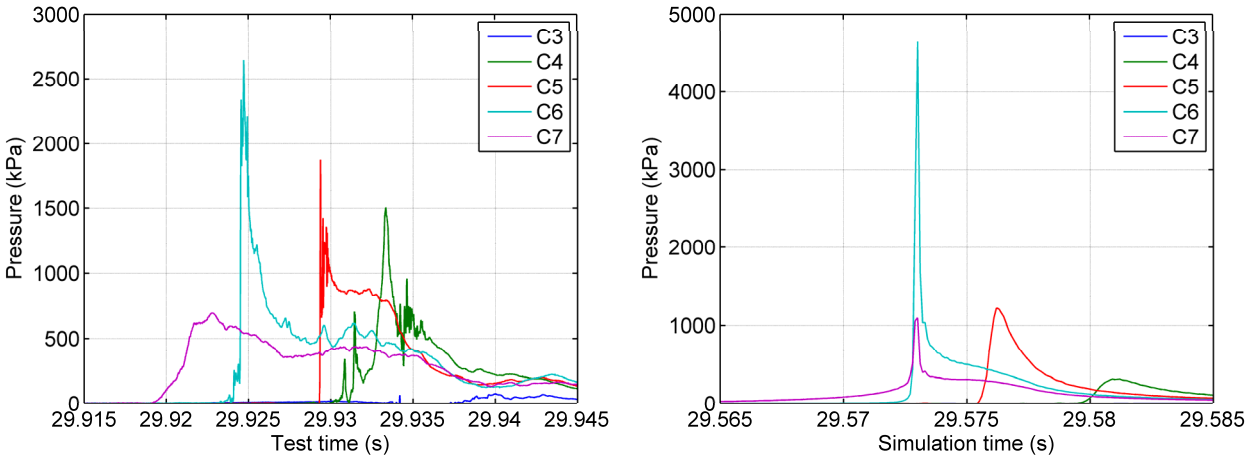

Figure 4. Pressure evolution for a flip-through impact at five locations aligned vertically. On the left, experimental recording for which each location (C3 to C7) corresponds to a sensor. On the right, numerical results at locations corresponding to experimental ones.

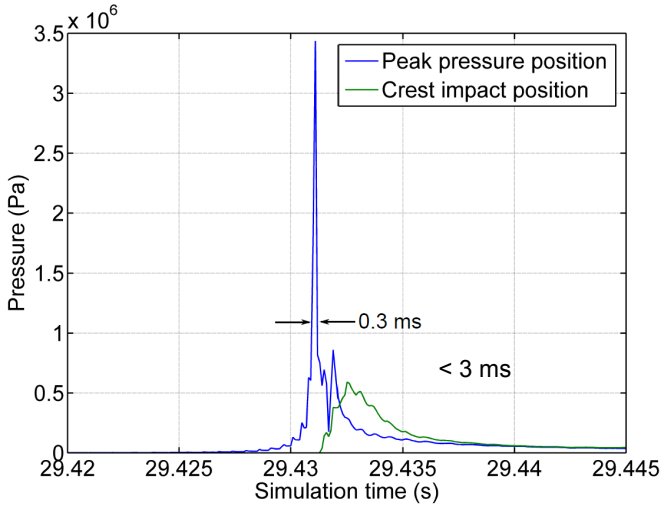

Figure 5. Time history of the pressure recorded on the wall at z=3.95 m (peak pressure position, in air-pocket region) and at z=4.05 m (wave crest impact position) for a violent incompressible impact involving a large air-pocket.

On the other side, compressible numerical results and experimental peak pressures are much more similar for this type of impact. It tells us that for impacts involving air entrainment, it is essential to consider compressibility effect. Otherwise, the energy of the impact is artificially released instantaneously which leads to overestimate pressures and forces on the wall. With compressibility effects, pressure rise is damped and spread on a longer time lapse (pressure peak is 3 ms instead of 0.3 ms), as illustrated in Figure 6. This figure also shows different oscillations in the pressure evolution. After performing a FFT on the signal, the frequency contents is mainly between 2 and 10 Hz with a peak around 5 Hz. These oscillations may be associated to the "vibration" of the air-pocket during and after the impact. Using the actual geometrical characteristics of the air-pocket within the theoretical model proposed by Topliss *et al.* (1992), the oscillation frequency should be around 8-9 Hz which is fairly close to the numerical results. Fast oscillations in the order of 200 Hz can also be observed during the first 50 ms. Their origin is not determined yet, but it could merely be something in the numerics.

Unfortunately, no small air-pocket impact has been obtained within the simulations (see Figure 7). This aspect would be interesting to test in order to check if the compressibility effects are as much important for low aeration impact since there is less air to compress. Moreover, it should be noted that, unlike the flip-through impact, air-pocket impacts show similar air-pocket shape and size in both compressible and incompressible flow simulations. Sloshing impacts have not been conducted in compressible flow because it was expected that a non-breaking wave should not undergo compressibility effects.

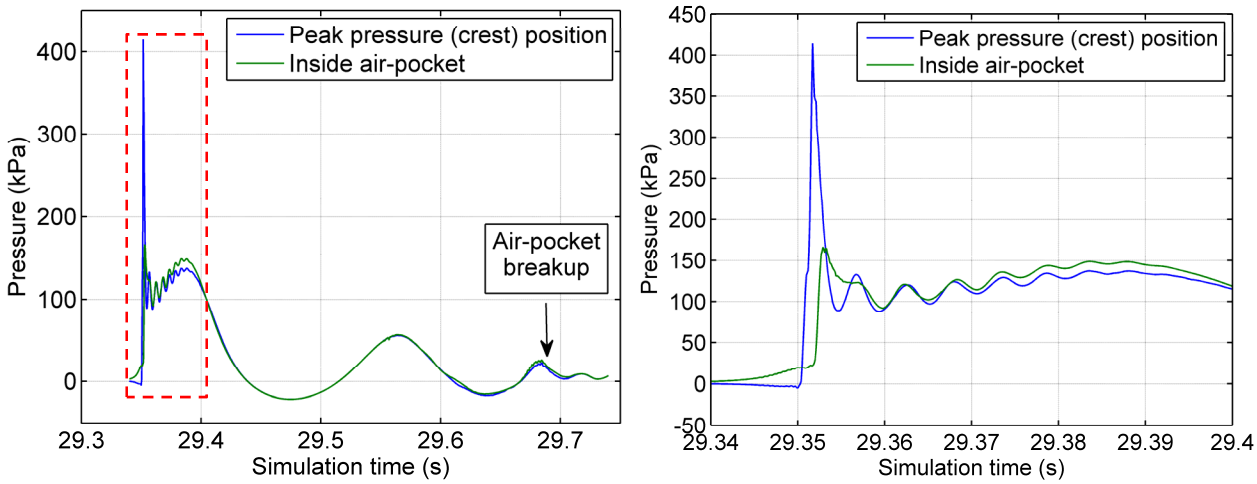

Figure 6. Pressure time history recorded on the wall at z=4.03 m (peak pressure position, at the crest) and at z=3.93 m (inside the air-pocket) for a violent compressible impact involving a large air-pocket. The right graph is a zoom.

When computing the pressure integral on the wall, we observe that the total horizontal distributed force (force on unitary width) for the incompressible large air-pocket case reaches 4300 kN/m. This enormous force, compared with Cuomo *et al.* (2010) and Hofland *et al.* (2010), is due, as explained above, to the unsuitable high pressure inside the air-pocket. Indeed, a more realistic force is obtained with the model involving compressibility, that is 250 kN/m. However, it is not the highest force calculated with the model: the compressible flip-through impact yields a maximum total horizontal force of 1150 kN/m. This force is maintained only during 1 ms.

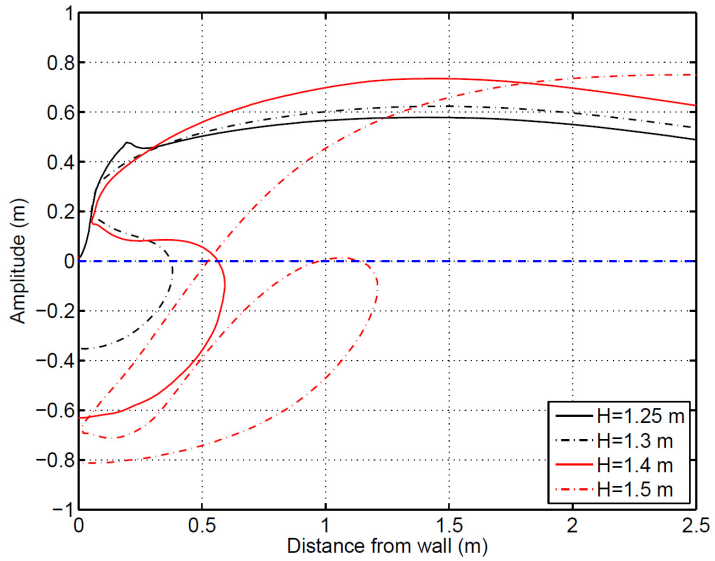

Figure 7. Wave surface profiles during the impact at the wall for all cases involving an air-pocket (H=1.3, 1.4, 1.5 m) and for a flip-through case (H=1.25 m). No small air-pocket impact has been obtained.

As well, integral may be done over time, which gives the pressure impulse. Cooker *et al.* (1995) developed an analytical model assuming incompressible and irrotational flow able to predict the pressure impulse generated by a wave impact. A comparison with this model is done in Figure 8 for the flip-through impact (assuming the same wave height and crest velocity), which is known to be roughly irrotational. Numerical and analytical curves are similar in shape and in amplitude, with a little overestimation by the numerical model. Differences may be explained by the fact that the analytical model assumes uniform and horizontal velocities under the wave. Compared to the experimental curve, both underestimate the pressure impulse. Despite the fact that each of them has the same crest velocity, the experimental wave has a greater height and thus has more energy. Then, even if the experimental peak pressure is smaller (Figure 4), the pressure impulse is bigger. Integrating the pressure impulse over the height gives the force impulse. The numerical flip-through generates an impulse of 4.27 kN.s/m whereas the analytical model predicts an impulse of 3.81 kN.s/m. The experimental pressure impulse profile is incomplete, but it may give an impulse bigger than 8 kN.s/m.

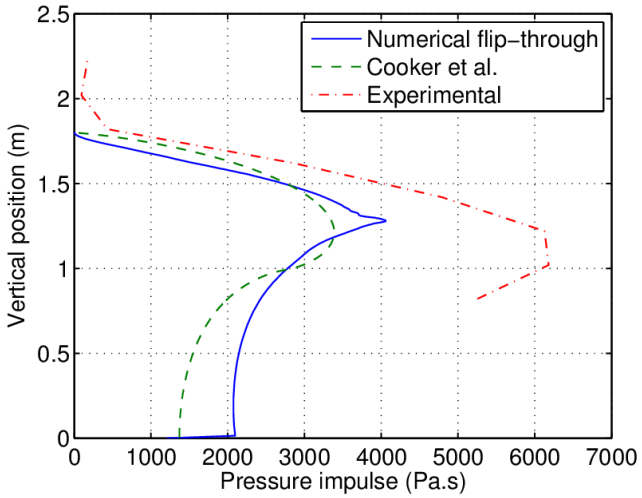

Figure 8. Comparison between the compressible numerical flip-through, the experimental one (8 data points) and the Cooker *et al*. model for the pressure impulse along the wall.

For design purposes (e.g. deflectors, wall shapes, road systems), it is also important to report maximum velocities along the seawall. Table 4 presents preliminary results of maximum local instantaneous water jet velocities near the wall after impact. Those velocities are measured above the point involving maximum pressure, bellow the top of the wall and are rounded to the nearest 5 m/s. It was found from the present limited tests that jet velocity in the order of 125 m/s is possible during a brief period (about 1 ms), when the jet is forming (and where it would have been difficult for a camera to capture it). At this point in the experimental study (preliminary results), a 40 m/s has been identified above the wall with a 120 fps camera.

Table 4. Maximum instantaneous local water jet velocity near the wall obtained from compressible flow simulations. Values are rounded to the nearest 5 m/s.

Type of impact	V_{max}	
	Incompressible	Compressible
	[m/s]	[m/s]
Sloshing	40	-
Flip-through	105	125
Air-pocket	80	25

It can also be seen that the impact showing the highest jet velocity is the flip-through impact. To achieve high velocities, it does not need only high local pressure but also important pressure gradients. Flip-through impacts present those pressure gradients (Peregrine, 2003). Figure 9 illustrates this point. A very high localized pressure point under a low pressure region accelerates the incoming fluid upward generating a fast jet. This phenomenon can also be understood by the fact that the "free-surface point" on the wall must go upward very fast since the wavefront is almost vertical.

In addition, one can see that the maximum velocity for the air-pocket impact in the compressible case is far less than the incompressible case. In fact, the maximum velocity may be linked to the peak pressure on the wall since the pressure reached in the compressible case is also much lower. Likewise, the increase in pressure for the flip-through impact is followed by an increase in maximum velocity. However, the sloshing impact sustains non-negligible jet velocity (it is assumed that compressible and incompressible simulations present similar maximum velocities since compressibility effects do not play a major role in this type of impact) despite the fact that it undergoes low wall pressures. It thus points out that jet velocity is not necessarily correlated with peak pressure.

5 CONCLUSIONS

This study aims to investigate the behavior of an idealized seawall following wave impacts using a numerical model. Fluid dynamics is in fact simulated to get inputs for structural analysis and deflector design, and to get insight of the wave impact physics. Then, the first step is to develop a numerical model that can reproduce results obtained from large scale impacts in our laboratory flume.

A 2D compressible flow model based on Navier-Stokes equation is used here to study compressibility effects and to reproduce different impacts observed in the experiments. Despite the amplitude of the more violent impact, the

compressible numerical model shows the same trends compared to the experimental tests according to the impact type. The maximum wall pressure obtained in the preliminary calculations is 4.6 MPa and is higher than those recorded in the large scale experiments (3.3 MPa), but both follow similar time evolution and spatial distribution. Furthermore, the numerical model captures physical phenomena and characteristics predicted by analytical models such as air-pocket oscillations and pressure impulse. Thus, although the model needs more comparison points and validation cases, it is able to reproduce and describe interesting characteristics of flip-through impacts or air-pocket impacts. Numerical results also depict interesting physics around the water jet, presenting substantial velocity magnitudes in the order of 100 m/s. These values need more validation.

In future work, to get design input for new large scale experiments, run up heights and overtopping quantities from the numerical simulations will be investigated. Different wave periods and depths will also be tested. Deflector numerical modeling is an interesting avenue in coastal design and should be address in order to support large scale experiments. Finally, 3D simulations are planned in the future to check if there are any effects of the flow nonuniformity in the width (whereas the flow is overall two-dimensional) on the resulting pressures and forces on the wall.

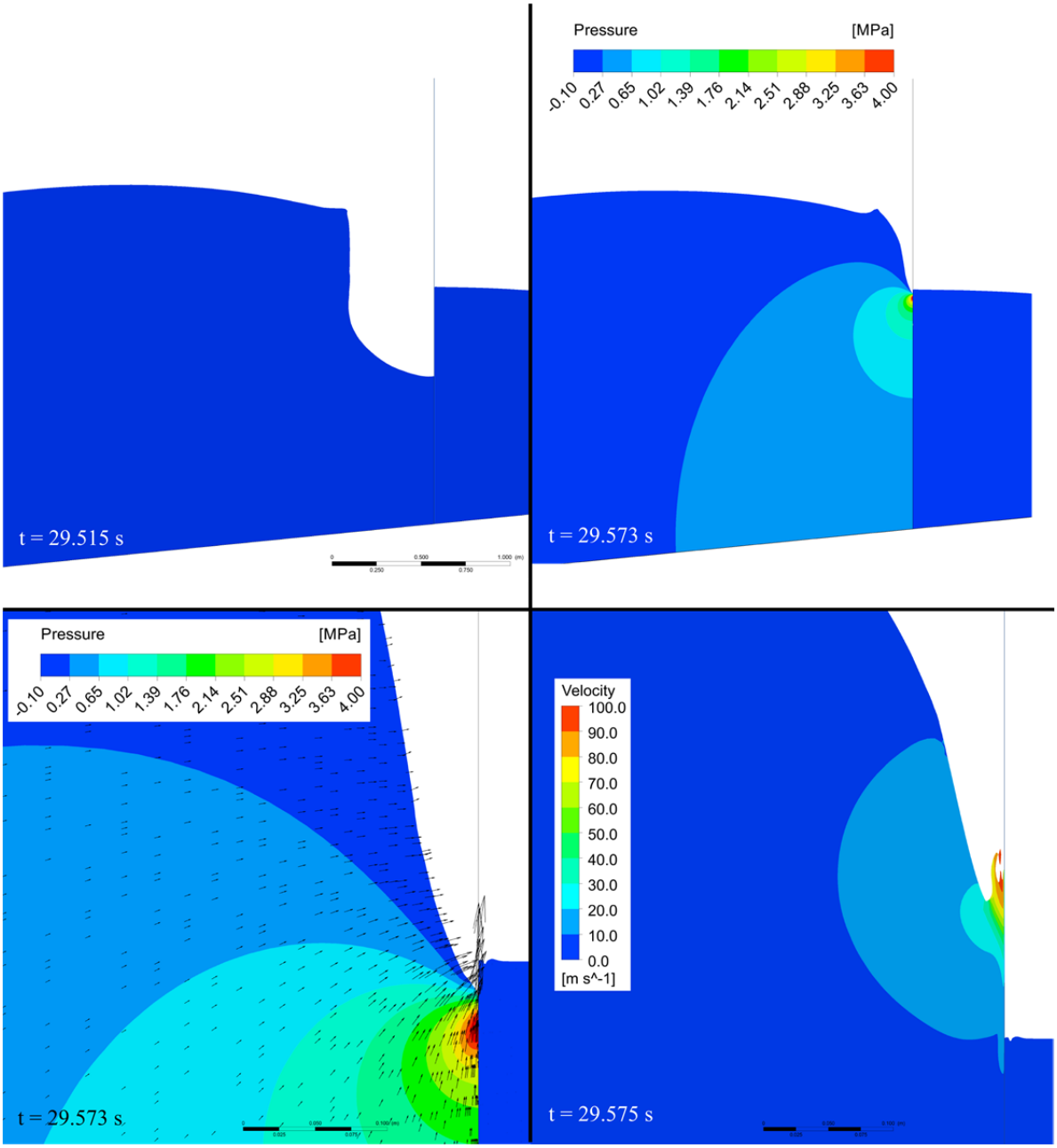

Figure 9. Pressure and velocity contours across a flip-through impact (compressible flow) at different instants. Some velocity vectors are added to show direction and acceleration of the water due to important pressure gradients.

ACKNOWLEDGEMENT

The present project is supported by le ministère des Transports du Québec, through the funding of the Research Chair in Coastal and River Engineering, and by the INRS - Centre ETE. Also, special thanks to Yves Gratton as well as Calcul Québec for having provided us the computing resources and to laboratory staff for having made possible the validation material from the large scale tests: Régis Xhardé, Francis Bérubé, Louis-Francois Rinfret and Gino Fontaine.

REFERENCES

ANSYS Inc., 2014. ANSYS Fluent 15.0 User's Guide.

Bagnold, R., 1939. Interim report on wave-pressure research, *Proc. Inst. Civil Eng*., 12, pp. 201–226.

Bredmose H., Peregrine D.H., Bullock G.N., 2009. Violent breaking wave impacts. Part 2: modelling the effect of air, *Journal of Fluid Mech*anics, vol. 641, pp. 389-430.

Bullock G.N., Obhrai C., Peregrine D.H., Bredmose H., 2007. Violent breaking wave impact. Part 1: Results from large-scale regular wave tests on vertical and sloping walls, *Coastal Engineering*, 54, pp. 602-617.

Cooker, M. and Peregrine, D., 1995. Pressure-impulse theory for liquid impact problems, *J. Fluid Mech*., 297, pp. 193–214.

Cuomo, G., Allsop, W., Bruce, T. and Pearson, J., 2010. Breaking wave loads at vertical seawalls and breakwaters, *Coastal Engineering*, 57, pp. 424–439.

Frandsen, J. B. and Berube, F., 2015. Large scale experimental wave impact on walls in the Quebec Coastal Physics Laboratory, *In Proceedings of ASME 2015 34th International Conference on Ocean, Offshore and Arctic Engineering,* 7, 10 p.

Frandsen, J. B., Tremblay, O.G. and Xhardé, R.., 2016. Investigations of wave impact on walls, *In Proceedings of 6th International Conference on the Application of Physical Modeling in Coastal and Port Engineering and Science (Coastlab16),* 10 p.

Guilcher P., Jus Y., Brosset L., Scolan Y. and Le Touze D., 2014. 2D Simulation of breaking wave impacts on a flat rigid wall – Part 1: influence of the wave shape, *The International Society of Offshore and Polar Engineers (ISOPE),* pp. 232-245.

Hattori, M. and Tsujioka, N., 1996. Dynamic response of vertical elastic walls to breaking wave impact, *In Proceedings of 25th Conference on Coastal Engineering*, pp. 2456–2469.

Hirt, C. and Nichols, B., 1981. Volume of fluid (VOF) method for the dynamics of free boundaries, *Journal of Computational Physics*, 39(1), pp. 201 – 225.

Hofland B., Kaminski M.L. and Wolters G., 2010. Large scale wave impacts on a vertical wall, *In Proc. of 32nd Conf. on Coastal Eng*.

Khayyer, A. and Gotoh, H., 2009. Modified moving particle semi-implicit methods for the prediction of 2d wave impact pressure, *Coastal Engineering*, 56(4), pp. 419 – 440.

Launder, B. and Spalding, D., 1974. The numerical computation of turbulent flows, *Computer Methods in Applied Mechanics and Engineering*, 3(2), pp. 269 – 289.

Lighthill, J., 1986. Fundamentals concerning wave loading on offshore structure, *J. Fluid Mech*., 173, pp. 667–681.

Mayer, S., Nielsen, K. and Hansen, E., 2005. Numerical prediction of wave impact loads on multiple rectangular beams, *Coastal Engineering Journal*, 47(1), pp. 41–65.

Mokrani, Cyril, Abadie, Stéphane and Zibouche, Kamel, 2013. Lien entre la forme locale de la surface libre et les pressions d'impact générées par une vague déferlante sur un ouvrage, *La Houille Blanche(6)*, pp. 53–57.

Peregrine, D., 2003. Water-wave impact on walls, *Annual Review of Fluid Mech*anics, 35, pp. 23–43.

Sarpkaya, T., 2010. *Wave Forces on Offshore Structures*, Cambridge University Press. 9781107461161.

Topliss, M., Cooker, M. and Peregrine D., 1992. Pressure oscillations during wave impact on vertical walls, *In Proceedings of 23rd International Conference on Coastal Engineering*, pp. 1639-1650

Tremblay, O. G. and Frandsen, J. B., 2015. 2D Numerical viscous prediction of wave impact effects on an idealized seawall rooted in large scale experiments (1:4), *In Proceedings of ASME 2015 34th International Conference on Ocean, Offshore and Arctic Engineering,* 7, 12 p.